Available online at www.sciencedirect.com
ScienceDirect
ELSEVIER
Ultramicroscopy 107 (2007) 543–550
ultramicroscopy
www.elsevier.com/locate/ultramic

Application of a 2-beam model for improving the structure factors from precession electron diffraction intensities

Wharton Sinkler[a,*], Christopher S. Own[b], Laurence D. Marks[b]

[a]UOP LLC, Des Plaines IL 60017, USA
[b]Department of Materials Science and Engineering, Northwestern University, Evanston IL 60201, USA

Received 19 January 2006; accepted 22 February 2006

Abstract

A 2-beam model is used to simulate precession electron diffraction (PED) intensities. It is shown that this model can be inverted with minimal knowledge of the underlying crystal structure, permitting structure factor amplitudes to be deduced directly from measured intensities within the 2-beam approximation. This approach may be used in conjunction with direct methods to obtain correct, kinematically interpretable structure indications for data sets from relatively thin crystals (less than approximately 400 Å), and an experimental example based on $(Ga,In)_2SnO_5$ is presented. The failure of this approach at large thickness is illustrated by an additional data set for MFI zeolite. The 2-beam approximation provides a simple model for PED intensities, and inversion using this model shows advantages over a kinematical approximation. It is however too rough approximation to be of general use and ultimately it is to be hoped that more accurate models with similar ease of use can be derived to treat PED data.

Keywords: Precession electron diffraction; Electron crystallography; Zeolite

1. Introduction

It is well known that the use of transmission electron diffraction (TED) for crystal structure analysis is hampered by the difficulty of interpreting intensities because of the effects of dynamical diffraction. Only in the limited case of extremely thin crystals is it strictly valid to use the kinematical approximation that the diffraction amplitudes (the square roots of the intensities) are the Fourier coefficients of the projected unit cell's structure, or structure factors. In the more general case the intensities in experimental data are the result of coherent multiple scattering, and reflections which are kinematically forbidden may become quite strong while those which are kinematically strong may be weak. Attempts to invert or undo the effects of multiple scattering to obtain directly interpretable structural information by restoring either the exit wave or the structure factors have so far met with limited practical success in terms of structure solutions of unknown phases [1–3].

While direct and rigorous inversion of multiple scattering has not proven successful in practical application, there are some approximations which, combined with careful experimentation, can yield usable data. The first of these is the kinematical approximation mentioned above, which has been used with electron diffraction data in a number of cases to solve crystal structures, particularly in cases of biological structures obtainable as very thin molecular crystals [4,5]. While this approach is attractive due to its simplicity and may succeed in light-element structures, it tends to fail for structures with elements heavier than oxygen and so it is not very useful for researchers in materials science or inorganic chemistry. Another approach is the 1 s channeling approximation [6–8], by which it has been shown that in some cases there is a simple relationship between diffraction intensities in a zone axis pattern and the projected crystal structure, specifically the diffraction amplitudes may represent the Fourier coefficients of a distribution with peaks at one or more subsets of

*Corresponding author.
E-mail address: wharton.sinkler@uop.com (W. Sinkler).

0304-3991/$ - see front matter © 2006 Elsevier B.V. All rights reserved.
doi:10.1016/j.ultramic.2006.02.008

the atom positions [9]. In some other cases the Σ_1 and Σ_2 distributions may be statistically obeyed [10,11], even though they may not be rigorously correct. However the condition for using 1 s channeling is that the projected structure consist of well-separated atom columns (in effect requiring some foreknowledge of the structure) and the subset of positions indicated in the data cannot be predicted without accurate knowledge of the sample thickness and detailed knowledge of the densities of the atoms in the columns.

Precession electron diffraction (PED) represents an experimental approach to obtaining more tractable diffraction intensities using electrons. PED was first described and performed by Vincent and Midgley in 1994 [12]. It grew out of the fact that higher-order Laue zone (HOLZ) reflections in large angle convergent beam electron diffraction (CBED) are near kinematical because of the relative absence of close multiple scattering vectors for these generally weak high-angle reflections [13]. In the precession technique the incident beam used typically has a small convergence, and is precessed or rotated around the surface of a cone centered on a zone axis direction (see Fig. 1). Because the beam avoids the exact zone axis direction (which is generally the most dynamical condition) the perturbations due to multiple scattering are expected to be less severe. An added benefit is that the precession will swing the Ewald sphere through the reciprocal lattice points thus allowing integrated intensities to be measured, and also reducing the sensitivity to minor tilt misorientations. These benefits have led to increasing application of PED in electron crystallography [14–20].

In spite of the reduction of the effects of multiple scattering, recent work clearly shows that the precession intensities cannot generally be treated as approximately kinematical [15]. The question then is whether the precession intensities can be treated using approximations, in any way which will make them reliably useful for structure analysis, where reliable might mean obtaining usable structure indications from routine direct methods 90% of the time for patterns taken with care on a thin area but not requiring extraordinary skill or sample preparation efforts. One approximation which was suggested early in the literature on precession is a 2-beam approach [12,21], reasonable because the effect of precession is to reduce the number of simultaneously excited beams and the limit of this is the 2-beam case in which the $\mathbf{g} = 0$ beam and one diffracted beam are excited. It has also been pointed out that if 2-beam theory can be applied and if one assumes that the integration is complete, a treatment for powder diffraction developed by Blackman [22] would be applicable to PED [14]. The current work explores the question of whether a 2-beam approximation can be used to give an approximate inversion of experimental data without the need for a forward calculation. We demonstrate that at least for a reasonably thin sample it can.

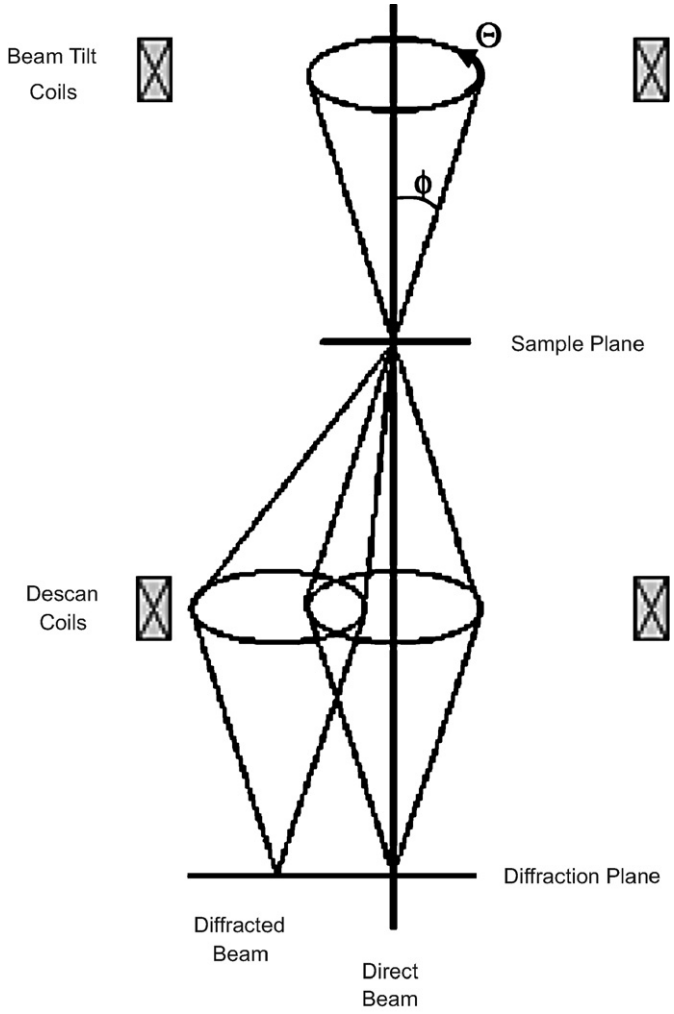

Fig. 1. Schematic depiction of the precession technique. Beam tilt coils above the sample scan the incident beam along the surface of a cone with semi-angle φ (varying Θ as a function of time). Reflections rotate along circles in the back focal plane (level of descan coils). The descan coils compensate for circular rotation and result in stationary measurable point reflections in the diffraction plane.

2. Two-beam forward calculation applied to precession g

A short recap of the relevant 2-beam theory is appropriate. In the case of excitation of a single Bragg reflection, the 2-beam intensity $|\phi_g(t)|^2$ for the beam at reciprocal lattice vector $\mathbf{g}$ is given by [23]

$$|\phi_g(t)|^2 = 1 - |\phi_0(t)|^2 = \left(\frac{\pi}{\xi_g}\right)^2 \frac{\sin^2 \pi t s_{\text{eff}}}{(\pi s_{\text{eff}})^2} \tag{1}$$

where ξ_g is the extinction distance (given by $\pi V_c/(\lambda F_g)$, with V_c the unit cell volume) for the reflection at reciprocal lattice vector $\mathbf{g}$, t is the sample thickness, $\phi_0(t)$ is the amplitude of the beam at $\mathbf{g} = 0$ and s_{eff} is given by $\sqrt{s^2 + 1/\xi_g^2}$, where s is the excitation error. In the case of PED, illustrated in Fig. 1, the electron beam is swung about a cone with semi-angle φ as the angle Θ is varied from 0 to 2π. For an instantaneous value of Θ it can be

shown (e.g. [21]) that the excitation error s for the beam at **g** is given by

$$s = -\frac{g^2}{2k} + g\varphi \cos\theta, \tag{2}$$

where $k = 1/\lambda$ and g is $|\mathbf{g}|$, the spatial frequency. In the 2-beam approximation (assuming that the convergence is small and has negligible effect), the precession intensity is thus given by

$$I_{2\text{beam}}(\mathbf{g}) = \frac{1}{2\pi}\left(\frac{\pi}{\xi_g}\right)^2 \int_0^{2\pi} \frac{\sin^2 \pi t s_{\text{eff}}(\theta,)}{(\pi s_{\text{eff}}(\theta))^2}\, \mathrm{d}\theta \tag{3}$$

In the limit where the semi-angle becomes infinitely large this will approach the Blackman formula, and approximations to Eq. (3) were developed by Gjønnes [21]. A more comprehensive analysis of the limits for which these approximations hold for fully dynamical diffraction will be published elsewhere [24]. Here we seek to establish that the full numerical form of Eq. (3) is a reasonable approximation by comparing it to the results of a full dynamical multislice approach (for details of the multislice see Ref. [25]). The comparison is shown in Fig. 2, which plots the 2-beam intensities from numerical integration of Eq. (3) against the multislice intensities for a variety of thicknesses for $(Ga,In)_2SnO_4$ [26] in [0 1 0] orientation. As can be seen, use of the 2-beam approximation provides reasonable scaling with the multislice simulations up to a thickness of approximately 200 Å. By using an agreement factor describing the scatter in plots such as shown in Fig. 2, it is possible to quantify the extent of agreement between a 2-beam approximation and the full dynamical multislice PED calculations. For this purpose, we define an R-factor as

$$R = \frac{\sum_g |I_{g,\text{MS}} - aI'_g|}{\sum_g I_{g,\text{MS}}}. \tag{4}$$

In which $I_{g,\text{MS}}$ is the multislice calculated intensity for the beam at **g** and I'_g is the fitted intensity (for example the 2-beam intensity), and a is a constant adjusted to minimize R. A plot of this R-factor versus thickness for several different precession tilt semi-angles is shown in Fig. 3a for the case of 2-beam calculated PED intensities from Eq. (3). As a comparison, kinematical simulated precession intensities were also calculated as a function of thickness by replacing s_{eff} with s in Eq. (3). Note these kinematical PED intensities implicitly include the adjustments for precession

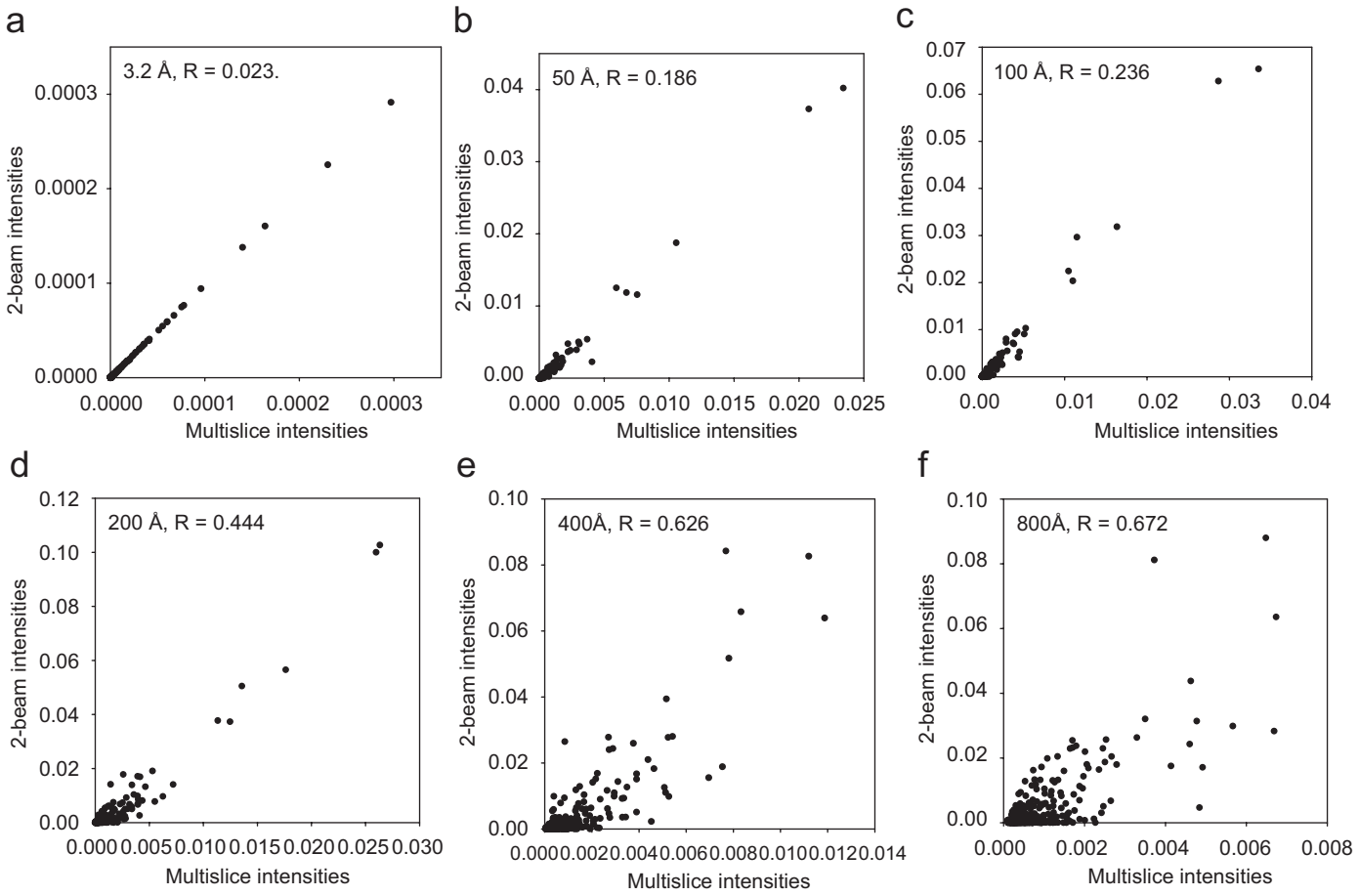

Fig. 2. Plot of simulated 2-beam PED intensities against multislice simulated PED intensities for $(Ga,In)_2SnO_5$ in [0 1 0] projection at a semi-angle $\varphi = 36$ mrad. Multislice calculations were performed in all cases with 1000 sampling steps, to 1.5 $Å^{-1}$ resolution. Plots are for a range of thicknesses. Values for R shown were calculated using Eq. (4).

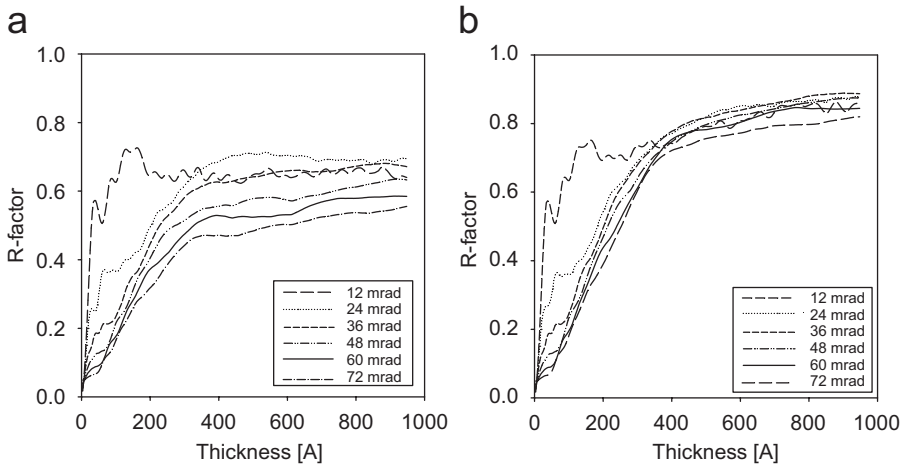

Fig. 3. Plots of *R*-factor vs. thickness from Eq. (4) for fit of (a) simulated PED 2-beam intensities and (b) simulated PED kinematical intensities for $(Ga,In)_2SnO_5$ [0 1 0] zone axis pattern. For both the 2-beam and kinematical calculations, the precession geometry is accounted for via Eq. (3) (with s_{eff} set to equal s for kinematical). The plots show the influence of both thickness and cone semi-angle φ on agreement.

geometry discussed by previous authors [12,21]. It is clear from these plots that the 2-beam approximation, although it is of limited accuracy, nevertheless provides a better match with full dynamical simulations than does the kinematical-based PED calculation.

3. Inversion of 2-beam precession intensities to structure factors

The above section illustrates that a 2-beam approximation can provide a modest but real improvement over kinematical theory for modeling precession intensities. The importance of the 2-beam approximation, where it may be valid, is that its forward calculation requires significantly weaker knowledge of the crystal structure than a full dynamical calculation (multislice or Bloch wave). In particular, as was recognized by Gjønnes et al. [18], it is not necessary to know the structure factor phases (or the atom positions), but merely the structure factor amplitudes (or the equivalent extinction distances ξ_g). Assume for the moment that the sample thickness is known or can be estimated, and that a single extinction distance ξ'_g in the data set is known. It is now possible (provided knowledge of φ for the experiment) to compute the intensity of the known beam at $\mathbf{g}'$ and compare this with the experimentally measured intensity to obtain a scaling factor

$$C_{\text{pattern}} = \frac{I_{\text{calc}}(\mathbf{g}')}{I_{\text{exp}}(\mathbf{g}')}. \tag{5}$$

Once C_{pattern} has been derived all the experimental intensities can be rescaled by multiplying with C_{pattern} such that

$$I_{\text{sca}}(\mathbf{g}) = C_{\text{pattern}} \times I_{\text{exp}}(\mathbf{g}) \tag{6}$$

Using the known or estimated thickness, the value of ξ_g^{-1} may be varied in calculating $I(\mathbf{g})$ via Eq. (3) until a match to $I_{\text{sca}}(\mathbf{g})$ is obtained. Using this approach (relying on knowledge or reasonable estimation of two constants) the 2-beam model may is invertible to obtain the full set of ξ_g and thus the structure factor amplitudes (proportional to ξ_g^{-1}).

In practice, there is an additional complication due to non-uniqueness of ξ_g^{-1} for some intensity values. This is illustrated in Fig. 4a, which shows a plot of the 2-beam precession intensity as a function of ξ_g^{-1} for thicknesses of 200 and 400 Å and typical constant values of the other pertinent parameters. For fixed acquisition parameters (voltage, thickness and φ) these curves are fully determined for each reflection in the pattern by the value of $|\mathbf{g}|$. As expected from 2-beam theory the curves show oscillatory behavior with local minima at roughly positions $\xi_g^{-1} = n/t$. Beams with scaled intensities beyond the first minimum have multiple values of ξ_g^{-1}, so that it will be possible to match the observed intensity value with multiple structure factor values. As illustrated in Fig. 4a, this problem of ambiguity becomes more severe as the thickness increases. However, it should be pointed out that in the example of $(Ga,In)_2SnO_5$ at 200 kV the minimum extinction distance (4,0,−1) is 580 Å, (ξ_g^{-1}~0.0017) and values below 150 Å (ξ_g^{-1} above ~0.007 in Fig. 4b) will seldom if ever be encountered. For a 200 Å thickness there would thus be no ambiguity to ξ_g^{-1} for any reflection in the set.

Fig. 4b illustrates how the 2-beam precession intensity varies for different values of $|\mathbf{g}|$, and includes also the equivalent roughly parabolic curves for relrods described by a kinematical sinc function (Eq. (3) in which s_{eff} is replaced by s). It illustrates that for weak beams in a pattern the applied correction will be essentially a purely geometrical correction along the lines proposed by K. Gjønnes [21] depending only on the spatial frequency. For stronger beams the corrected value of ξ_g^{-1} from the 2-beam case will be larger than in the kinematical case, reflecting the drop off of intensity with thickness due to diffraction back into the incident beam in the 2-beam theory.

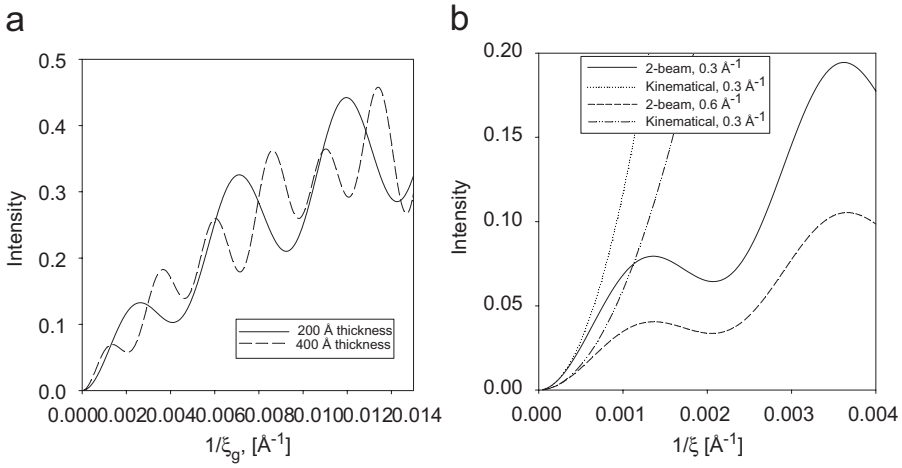

Fig. 4. (a) 2-beam intensity as a function of $1/\xi_g$ for a reflection at $|\mathbf{g}| = 0.34\,\text{A}^{-1}$, $\varphi = 36$ mrad, 200 kV, thicknesses of 200 and 400 Å. (b) 2-beam intensity and kinematical intensity as function of $1/\xi_g$ at constant 400 Å thickness, two different spatial frequencies 0.3 and $0.6\,\text{A}^{-1}$.

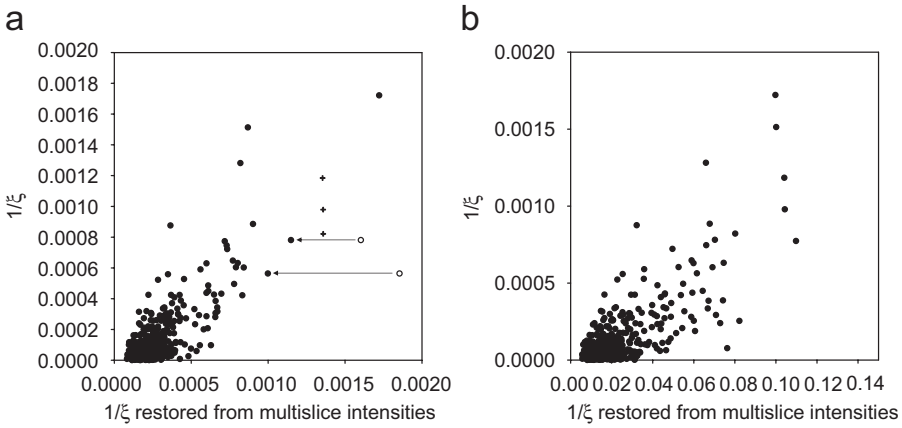

Fig. 5. (a) Two-beam based restoration of $1/\xi_g$ from multislice-simulated PED data for $(Ga,In)_2SnO_5$ [0 1 0] zone, 200 kV, 400 Å thickness, $\varphi = 48$ mrad. Plot compares restored values with $1/\xi_g$ calculated from structure. The + symbols are intensities which exceeded the first maximum in the plot of intensity vs. $1/\xi_g$ (see Fig. 4a) and were set to the $1/\xi$ value corresponding to the local maximum. The filled symbols are intensities lower than the first minimum (thus have only one root). Open symbols show 2nd root for the two beams in the set having multiple roots. (b) Kinematical-based restoration of $1/\xi_g$ using the same multislice input as for a).

The inversion of 2-beam intensities was performed on modeled multislice intensities for the case of $\varphi = 48$ mrad and 400 Å thickness, and Fig. 5a shows a plot illustrating the agreement between the restored ξ_g^{-1} and computed ideal ξ_g^{-1}. In spite of some outliers, a fairly linear tendency is seen in Fig. 5a, indicating that the restoration of extinction distances via a 2-beam approximation has provided some real benefit. For comparison to this Fig. 5b illustrates the degree to which kinematical structure factors would be approximated by using the parabola-like kinematical curves in Fig. 4b. This is clearly not a good approximation at 400 Å and $\varphi = 48$ mrad. For the two scatter plots in Figs. 5a and b respectively, the *R*-factors defined in Eq. (4) are 0.507 and 0.528, respectively.

4. Applications to experimental intensities

The inversion process was applied to experimental precession intensities for $(Ga,In)_2SnO_5$. The data, also presented in Ref. [25], were collected on a JEOL 2000FX TEM with a precession device described in Ref. [27]. Köhler illumination was used with a 10 μm condenser aperture, and the illuminated area was approximately 100 nm in diameter. The precession semi-angle φ was 24 mrad. The pattern was acquired with a Gatan US1000 CCD camera and intensities were quantified using a cross-correlation technique similar to that described in Ref. [28]. Fig. 6a shows the degree of scaling between the ξ_g^{-1} restored based on 2-beam theory and the calculated values of ξ_g^{-1}. The scaling appears quite satisfactory. Fig. 6b shows the result of an a priori direct methods calculation from fs98 software using the restored values of ξ_g^{-1} as input. In spite of an unrealistic buildup of potential at the unit cell corners, the solution reveals subsidiary maxima in good agreement with the cation positions of the true structure, shown schematically in Fig. 6b.

An additional precession data set was acquired using a recent installation of a precession device on a JEOL 3000F

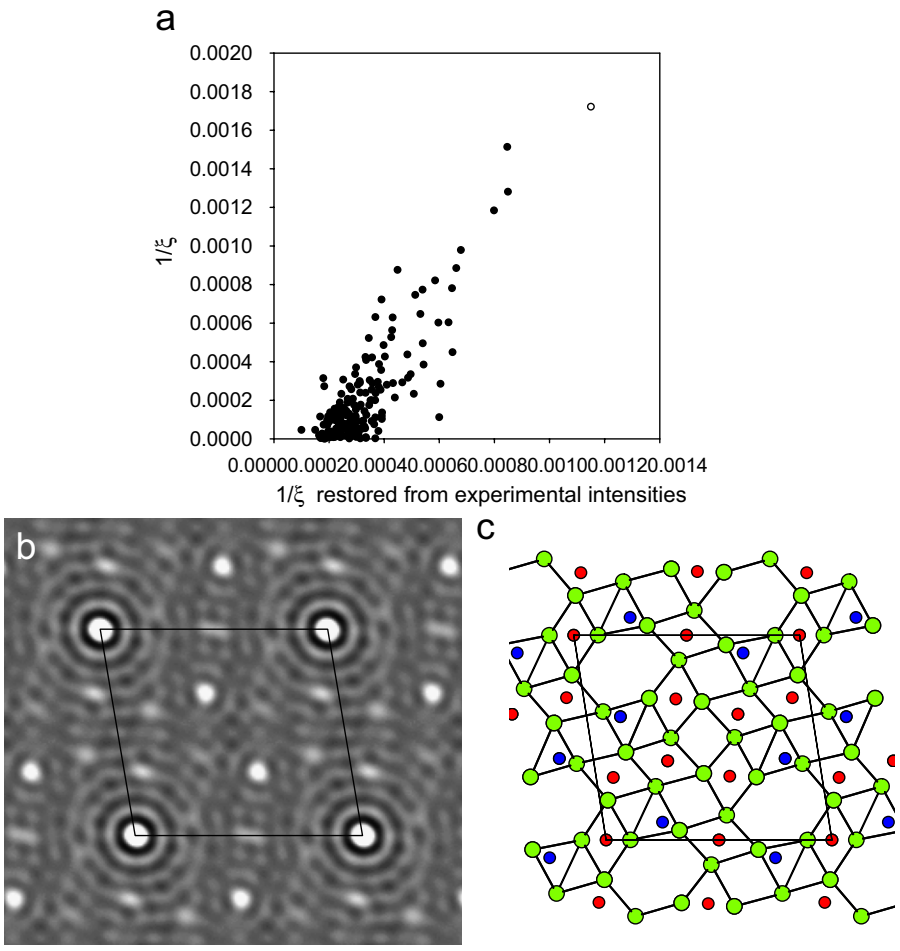

Fig. 6. (a) Restoration of $1/\xi_g$ using 2-beam inversion based on 475 Å, $\varphi = 24$ mrad experimental precession intensities. Open symbol represents a single reflection in the dataset which exceeded the first maximum of intensity vs. $1/\xi_g$ (see Fig. 4); since inversion would predict unrealistically large $1/\xi_g$ for this case value was set to first maximum of the appropriate plot, Fig. 4. (b) A priori direct methods solution using restored $1/\xi_g$ plotted in a). (c) Schematic of $(Ga,In)_2SnO_5$ viewed along [0 1 0]. Bonded atoms are oxygen, with cations lying in interstices. The cation positions have been restored in the direct methods solution.

field-emission TEM operating at 300 kV [29]. An MFI zeolite was oriented along the [0 1 0] zone axis which is also the direction of the primary straight pore system, and a pattern was acquired with a cone semi-angle φ of 33 mrad using Köhler illumination conditions similar to those described above. The raw data and reduction are shown in Fig. 7 and are compared with a map of the computed ξ_g^{-1} using atom positions from Ref. [30]. Also shown is the result of 2-beam inversion assuming a thickness of 1500 Å which is the refined thickness for the pattern based on comparisons with multislice simulations (see details in Ref. [25]). In this case only the strongest (5 0 1) beam had an ambiguous value of ξ_g^{-1}, but the larger root corresponds to an unrealistically short extinction distance (<10 Å). The 2-beam reconstruction is shown in Fig. 7d. Ideally, this should resemble the kinematical map (Fig. 7b), but in fact the differences are striking. By comparison with the experimental pattern in Fig. 7c the 2-beam based inversion has induced an overall flattening of the pattern by enhancing reflections at large spatial frequency relative to those near the origin. However it has not improved the loss of contrast between strong and weak beams which is an effect of dynamical many-beam interactions. Several varied attempts were made using direct methods to restore the MFI structure based on the data shown in Fig. 7, but none of the direct methods solutions contained reliable indications of the projected structure.

5. Discussion

PED provides several distinct advantages compared with standard TED or selected area electron diffraction. These advantages include better reproducibility because of integration of intensities and reduced sensitivity to tilt misalignment, as well as a less chaotic dependence of the intensities on thickness. Nevertheless, direct interpretability of the recorded intensities in terms of the underlying structure still presents serious challenges.

This paper has shown that an inversion process based on the 2-beam approximation has advantages over one using a simple kinematical approximation. Although the accuracy of the inversion is limited, particularly for thicker crystals,

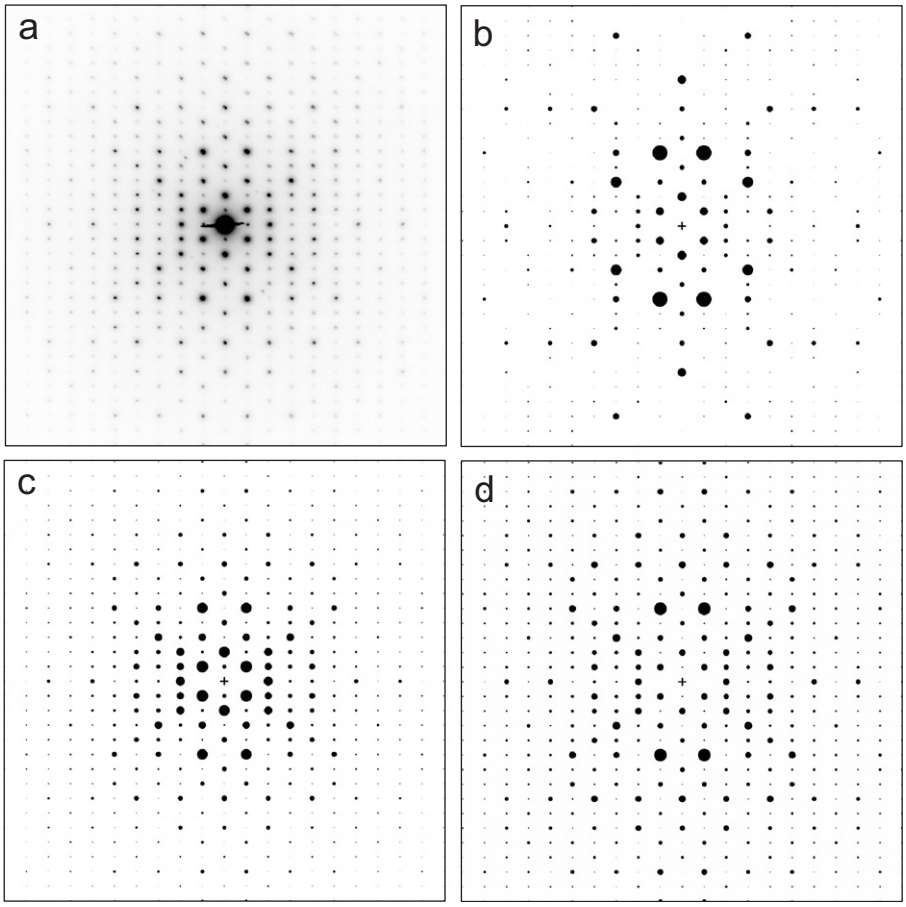

Fig. 7. (a) Experimental pattern, MFI [0 1 0] taken at 33 mrad, 300 kV. Vertical in pattern is the (h00) row. Note forbidden reflections for p2gg are present. (b) Computed map of $1/\xi_g$ (radii of circles proportional to $1/\xi_g$). (c) Quantification of (a), radii are square roots of intensities. (d) Two-beam based inversion of experimental intensities based on 1500 Å thickness (radii of circles are proportional to restored $1/\xi_g$).

the comparison between a 2-beam approximation and multislice calculations for $(Ga,In)_2SnO_5$ shows that in cases of relatively thin samples (<400 Å) and at large precession angles something resembling the multislice intensities is obtained with a 2-beam forward calculation. Because of its simplicity, the 2-beam model can (with some assumptions) be inverted to obtain ${\xi_g}^{-1}$ or the equivalent structure factors. For the condition of sufficiently thin sample, 2-beam theory may help to make PED more reliably applicable to crystallographic problems.

In its essence, the 2-beam inversion can best be understood based on Fig. 4. In relatively common cases where a second root is unlikely the correction amounts to a rescaling of the intensities using an S-shaped function (the $I(t)$ vs. ${\xi_g}^{-1}$ up to the first maximum in Fig. 4). This scaling is not completely straightforward, because the shape of the 'S' varies with spatial frequency, and gets shallower at larger spatial frequencies, also shown in Fig. 4. The essence of why this works involves how it effects strong and weak beams differently at a given spatial frequency: the strong beams near the top of the 'S' will be disproportionately emphasized (receive larger restored ${\xi_g}^{-1}$) and the weak beams will be reduced. This is thus effectively a spatial-frequency-dependent contrast enhancer of reflections, and it agrees with the general observation in precession electron diffraction that the intensities within a given spatial-frequency band are flatter and more equal than they are observed to be in kinematical simulations.

In the example given above for MFI zeolite, the 2-beam inversion is not sufficient to provide a usable set of ${\xi_g}^{-1}$ from precession intensities for this relatively thick crystal. However, it is not a foregone conclusion that nothing like a simple robust model of precession intensities exists which may make precession intensities from even thick samples more interpretable than they currently appear to be. This is reasonable primarily because of the existence of relatively simple rules of thumb as to how precession amplitudes differ from the corresponding kinematical structure factors. The primary attributes can be ascertained by comparison of Figs. 7b and 7c above, and may be summarized as (1) a damping of intensities away from the pattern's center and (2) an overall loss of contrast between weak and strong reflections within a given spatial frequency band. Beyond this there is a tendency for the intensities within a systematic row to all be strong whenever the first order beam in the row is strong

(also seen in Fig. 7b in the diagonal rows of (h0h) reflections). One starting point for robust modeling of PED data may be the Bethe dynamical potentials described in Refs. [18,31]; however, since the construction of the Bethe potentials requires knowledge of both structure amplitudes and their phases this approach needs to be modified to be made less model-dependent. The precession technique clearly provides a simpler and more reproducible form of electron diffraction. With the increasing availability of precession devices it may be hoped that further experimentation buttressed with careful theoretical work may be capable of arriving at an improved simple model for precession intensities, which, similar to the 2-beam approach presented here requires only weak knowledge in order to invert to reliable structure factor amplitudes.

Acknowledgments

The authors would like to acknowledge the support of UOP LLC for use of microscopes and support of precession instrumentation. Additional funding was provided by STCS, the US Department of Energy (Grant no. DE-FG02-03ER 15457), as well as Fannie and John Hertz Foundation (CSO).

References

[1] J.C.H. Spence, Acta Crystallogr. A 54 (1998) 7.
[2] L.J. Allen, T.W. Josefsson, H. Leeb, Acta Crystallogr. A 54 (1998) 388.
[3] W. Sinkler, in: G.W. Bailey, R.L. Price, E. Voelkl (Eds.), Microscopy and Microanalysis, Springer, Long Beach, CA, 2001, p. 1068.
[4] D.L. Dorset, Ultramicroscopy 38 (1991) 23.
[5] C.J. Gilmore, C.J. Nicholson, D.L. Dorset, Acta Crystallogr. A 52 (1996) 937.
[6] F. Fujimoto, Phys. Stat. Sol. 45 (1978) 99.
[7] D. Van Dyck, M. Op de Beeck, Ultramicroscopy 64 (1996) 99.
[8] W. Sinkler, L.D. Marks, J. Microsc. 194 (1999) 112.
[9] W. Sinkler, L.D. Marks, Ultramicroscopy 75 (1999) 251.
[10] F.N. Chukhovskii, J.J. Hu, L.D. Marks, Acta Crystallogr. A 57 (2001) 231.
[11] J.J. Hu, F.N. Chukhovskii, L.D. Marks, Acta Crystallogr. A 56 (2000) 458.
[12] R. Vincent, P.A. Midgley, Ultramicroscopy 53 (1994) 271.
[13] R. Vincent, D.M. Bird, Philos. Mag. A 53 (1986) L35.
[14] C.S. Own, A.K. Subramanian, L.D. Marks, Microsc. Microanal. 10 (2004) 96.
[15] J. Gjønnes, V. Hansen, B.S. Berg, P. Runde, Y.F. Cheng, K. Gjønnes, D.L. Dorset, Acta Crystallogr. A 54 (1998) 306.
[16] M. Gemmi, X. Xou, S. Hovmöller, A. Migliori, M. Vennstrom, Y. Andersson, Acta Crystallogr. A 59 (2003) 117.
[17] C.S. Own, W. Sinkler, L.D. Marks, Ultramicroscopy (2003).
[18] K. Gjønnes, Y.F. Cheng, B.S. Berg, V. Hansen, Acta Crystallogr. A 54 (1998) 102.
[19] P.A. Midgley, M.E. Sleight, M. Saunders, R. Vincent, Ultramicroscopy 75 (1998) 61.
[20] T.E. Weirich, J. Portillo, G. Cox, H. Hibst, S. Nicolopoulos, Ultramicroscopy 106 (2006).
[21] K. Gjønnes, Ultramicroscopy 69 (1997) 1.
[22] M. Blackman, Proc. Roy. Soc. A 173 (1939) 68.
[23] P.B. Hirsch, A. Howie, R.B. Nicholson, D.W. Pashley, M.J. Whelan, in: R.E. Krieger (Ed.), Electron Microscopy of Thin Crystals, Malabar, Florida, 1977.
[24] C.S. Own, W. Sinkler, L.D. Marks, (2007) in preparation.
[25] C.S. Own, L.D. Marks, W. Sinkler, Acta Crystallogr. A 62 (2006) 434.
[26] D.D. Edwards, T.O. Mason, W. Sinkler, L.D. Marks, K.R. Poeppelmeier, J.Sol. Stat. Chem. 150 (1997) 294.
[27] C.S. Own, L.D. Marks, W. Sinkler, Rev. Sci. Instrum. 76 (2005) 033703(1.
[28] P. Xu, G. Jayaram, L.D. Marks, Ultramicroscopy 53 (1994) 15.
[29] C. S. Own, Dissertation, Northwestern University, 2005.
[30] D.H. Olson, G.T. Kokotailo, S.L. Lawton, W.M. Meier, J. Phys. Chem. 85 (1981) 2238.
[31] J. Gjønnes, Acta Crystallogr. 15 (1962) 703.